

## High Efficiency Al-Free 980nm InGaAs/InGaAsP/InGaP Strained Quantum Well Lasers<sup>\*</sup>

XU Zun-tu(徐遵图), YANG Guo-wen(杨国文), ZHANG Jing-ming(张敬明),  
MA Xiao-yu(马骁宇), XU Jun-ying(徐俊英), SHEN Guang-di<sup>1</sup>(沈光地),  
and CHEN Liang-hui(陈良惠)

(Institute of Semiconductors, The Chinese Academy of Sciences, Beijing 100083, China)

(1 Beijing Optoelectronics Technology Laboratory and Department of Electronic Engineering,  
Beijing Polytechnique University, Beijing 100022, China)

**Abstract:** High efficiency Al-free InGaAs/InGaAsP/InGaP lasers emitting at 980nm are fabricated by MOCVD. The lasers exhibit a high internal quantum efficiency of 95% and a low internal loss of  $1.8\text{ cm}^{-1}$ . Low threshold current density of  $190\text{ A/cm}^2$  and high slope efficiency of  $1.06\text{ W/A}$  are obtained by lasers with  $800\mu\text{m}$  cavitylength. A high characteristic temperature  $210^\circ\text{C}$  is also obtained by replacing the GaAs barrier with high-bandgap InGaAsP barrier. The measured vertical and parallel divergence angle are  $40^\circ$  and  $8^\circ$ , respectively.

**Key words:** quantum well laser; high efficiency; Al-free

**PACC:** 4255P; 6855; 7856; 8115H

**CLC number:** TN248.4    **Document code:** A    **Article ID:** 0253-4177(2000)05-0417-04

### 1 Introduction

980nm InGaAs/GaAs/AlGaAs strained quantum well lasers have attracted considerable attention as pumping sources for the Erbium-doped fiber amplifiers (EDFA) and solid-state lasers<sup>[1,2]</sup>. However, for InGaAs/GaAs/AlGaAs strained quantum well lasers, the reliability is the most important because AlGaAs is acting as the cladding layers and waveguide layer in which optical fields are overlapped. Although catastrophic optical damage (COD), which used to be the major cause of failure, has now been largely overcome by the special surface passivation and facet AR/HR coatings, slow degradation still limits the lifetime to few  $\times 10^5$  hours due to the dark line defects in AlGaAs<sup>[3]</sup>. In order to overcome the reliability problem of AlGaAs-based 980nm lasers, Al-free 980nm

<sup>\*</sup> Project Supported by High Technology Research & Development Program of China (Contract No. 863-307-13-3).

XU Zuntu (徐遵图), male, was born in 1964, Ph. D., associater Professor. His research interests are in the areas of design and fabrication of III-V compound semiconductor lasers.

Received 12 December 1999, revised manuscript received 23 February 2000

strained quantum well lasers are developed with following main advantages<sup>[4,5]</sup>. (1) Less surface oxidation is expected due to Al-free during the fabrication process and laser operation, thereby, it reduces the recombination rate of laser facet. (2) InGaP cladding layers are of lower electrical and thermal resistance compared with AlGaAs cladding. (3) InGaAsP confinement layers give a better carrier confinement, consequently, high external quantum efficiency and high characteristic temperature  $T_0$  value are obtained compared with GaAs confinement layers. (4) Selective chemical etching between GaAs and InGaP gives precise control of the depth for fabricating ridge waveguide lasers.

The reports on InGaAs/GaAs/InGaP lasers<sup>[6]</sup> usually exhibit the low quantum efficiency because of the small conduction band offset at the GaAs/InGaP heterojunctions<sup>[7]</sup> and a weak carrier confinement, which results from a small energy separation between the quantum confined states and barrier potential. It is expected that the replacement of GaAs waveguide with an InGaAsP ( $> 1.5\text{eV}$ ) barrier and a waveguide layer or step graded index separate confinement heterostructure will improve the carrier injection efficiency and consequently enhance the internal quantum efficiency<sup>[8-10]</sup>. In this paper, we report a high efficiency InGaAs/InGaAsP/InGaP strained quantum well lasers in high output power.

## 2 Laser Structure and Material Growth

The InGaAs/InGaAsP/InGaP separate confinement heterostructure (SCH) of double quantum well laser structure is shown schematically in Fig. 1. The SCH active region consists of two 7nm-thick InGaAs strained-layer quantum wells with a 20nm

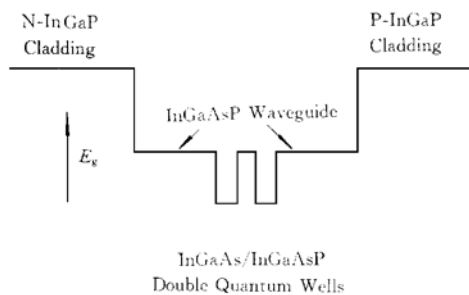


FIG. 1 Schematic Structure of InGaAs/InGaAsP/InGaP Lasers

In<sub>0.3</sub>Ga<sub>0.7</sub>As<sub>0.4</sub>P<sub>0.6</sub> (1.62eV, abbr. as InGaAsP) barrier layer sandwiched between two 420nm-thick InGaAsP broad waveguide layers. The n- and p-cladding layers are both 1.2μm-thick In<sub>0.49</sub>Ga<sub>0.51</sub>P (1.89eV, abbr. as InGaP). The higher bandgap of InGaP grown on exact (100) GaAs substrate provides a stronger carrier confinement, as should result in a relatively higher quantum efficiency and weaker temperature sensitivity (high  $T_0$  value) for our structure. The carrier

concentration of P<sup>+</sup>-GaAs ohmic contact layer is up to  $1 \times 10^{20} \text{cm}^{-3}$  in order to reduce the contact resistance. The laser structure is grown in an Aixtron AIX200 MOCVD system on a (100) n<sup>+</sup>-GaAs substrate. The growth temperature for the InGaP cladding layers and SCH active region is 680°C. The as-grown wafer has a mirror smooth surface morphology without any evidence of crosshatch or defects. The lattice mismatch of InGaAsP waveguide layers with GaAs substrate is controlled within  $\Delta a/a < 10^{-3}$ . Figure 2

represents a typical rocking curve of double crystal X-ray diffraction for InGaAsP-InGaP BW laser structure, from which, we can see that the  $\Delta a/a$  are  $8.06 \times 10^{-4}$  and  $1.1 \times 10^{-3}$  for InGaAsP and InGaP, respectively.

### 3 Device Performance

To characterize the performance of lasers, we fabricated the  $100\mu\text{m}$ -width stripe devices. The contact stripe, which is formed chemically by etching through  $p^+$ -GaAs cap layer outside the  $100\mu\text{m}$  wide stripe, prevents the current spreading and defines the metal contact stripe with a  $\text{SiO}_x\text{N}_y$  insulating layer. Ti/Pt/Au, and AuGeNi metals were evaporated to form ohmic contacts on p-type and n-type GaAs, respectively. The contacts were then alloyed at  $430^\circ\text{C}$  for 40s. For CW measurements, devices with a cavity length of  $800\mu\text{m}$  were coated (8%/98%) and mounted junction-side down on copper heatsinks. Figure 3 gives the light-current characteristics measured under CW condition at room temperature ( $25^\circ\text{C}$ ). The threshold current and slope efficiency are 150mA and 1.06W/A (83.8%), respectively. The relatively high efficiency is the results of low internal loss and high internal quantum efficiency caused by reducing the carrier absorption loss in broad-waveguide laser structure and improving the material quality. Figure 4 gives the relation between reciprocal of differential quantum efficiency and cavitylength. From this relation, we obtain the internal loss and internal quantum efficiency to be  $1.8\text{cm}^{-1}$  and 95%, respectively.

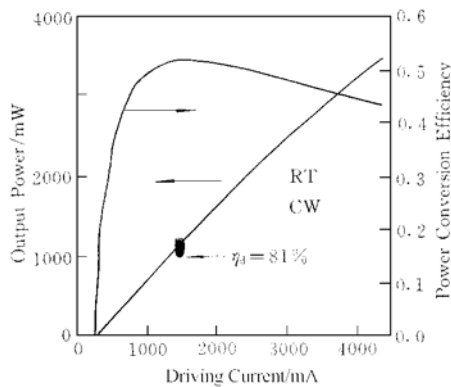


FIG. 3 Characteristics Measured Under CW Condition for InGaAs/InGaAsP/InGaP Broad Waveguide Lasers

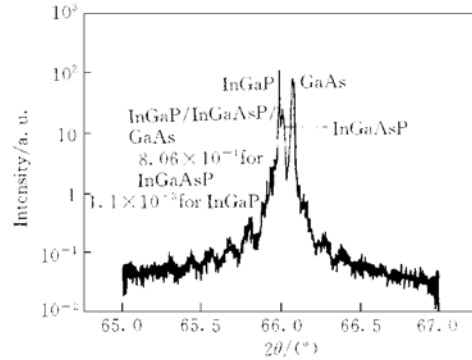


FIG. 2 Typical Rocking Curve of Double Crystal X-ray Diffraction for InGaAs/InGaAsP/InGaP Laser Structure

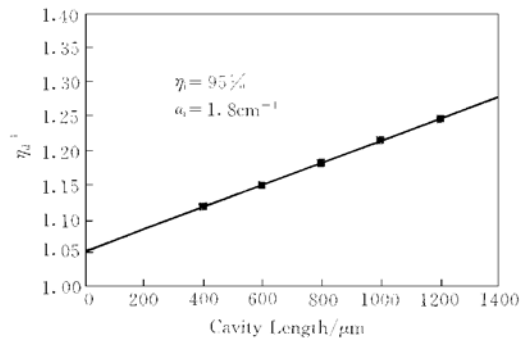


FIG. 4 Reciprocal of Differential Quantum Efficiency Versus Cavity Length

The maximum power conversion efficiency is 51% at an output power of 1.5W. The output power can reach 3.5W. The emission wavelength is 978nm at 1.0W. The vertical and parallel divergence angle are measured as 40° and 8°. The larger vertical divergence angle distributes to the strong optical confinement in the waveguide structure. It can be improved by the adoption of the multi-step InGaAsP waveguide or the replacement of InGaP cladding on AlGaAs.

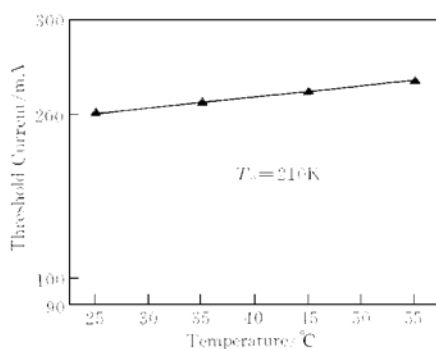


FIG. 5 Temperature Dependence of the Threshold Current over the Temperature Interval 25—55°C

Figure 5 shows the temperature dependence of the threshold current over the temperature interval 25—55°C, a high  $T_0$  value of 210K was obtained. The weak temperature dependence of the threshold current results from the application of two quantum wells and high bandgap InGaAsP (1.64eV) waveguide layers, which makes the carrier leakage from the InGaAs wells to the waveguide layers decreased at a higher temperature.

## 4 Conclusion

In conclusion, we have demonstrated that 980nm InGaAs/InGaAsP/InGaP strained quantum well lasers with broad waveguide structure exhibit a low threshold current density of 190A/cm<sup>2</sup> and high slope efficiency of 1.06W/A at 800μm cavity length. The internal quantum efficiency and internal loss are 95% and 1.8cm<sup>-1</sup>, respectively. A high characteristic temperature  $T_0$  of 210°C is obtained. High efficiency and high  $T_0$  distribute to the high quality material and strong carrier confinement by replacing the GaAs barrier with a high bandgap InGaAsP barrier. The maximum output power of 3.5W and power conversion efficiency of 51% are demonstrated.

## References

- [1] W. D. Laidig, P. J. Caldwell, Y. F. Lin and C. K. Peng, Appl. Phys. Lett., 1984, **44**: 653.
- [2] B. Pederson, B. A. Thompson, S. Zemon *et al.*, IEEE Photon. Technol. Lett., 1992, **4**: 46.
- [3] G. Grasso, F. Magistrali, G. Salmini, A. Oosenbrug *et al.*, OFC'95 Tech. Dig., 1995, **8**: 232.
- [4] Michio Ohkubo, Shu Namiki *et al.*, IEEE Journal of Quantum Electronics, 1993, **29**: 1932.
- [5] G. Zhang, J. Nappi *et al.*, Appl. Phys. Lett., 1992, **61**: 96.
- [6] Yang Guowen, Xu Zuntu, Ma Xiaoyu *et al.*, Chinese Journal of Semiconductors, 1998, **19**: 548 (in English) [杨国文, 徐遵图, 马晓宇, 等, 半导体学报, 1998, **19**: 548 (in English)].
- [7] M. A. Hasse, M. J. Hafich and G. W. Robinson, Appl. Phys. Lett., 1991, **58**: 616.
- [8] S. H. Groves, J. N. Walpole *et al.*, Appl. Phys. Lett., 1992, **61**: 255.
- [9] G. Zang, Electron. Lett., 1994, **30**: 1230.
- [10] Pekka Savolainen, Mika Toivonen *et al.*, IEEE Photon. Technol. Lett., 1996, **8**: 986.